Tribology Letters (2019) 67:35
https://doi.org/10.1007/s11249-019-1144-0

ORIGINAL PAPER

A Scratch-Guide Model for the Motion of a Curling Rock

A. Raymond Penner[1]

Received: 27 November 2018 / Accepted: 4 February 2019 / Published online: 22 February 2019

Abstract
A model based on a scratch-guide mechanism being responsible for the curl of a curling rock is presented. The model is based on the postulate that when the asperities around the rear of the running band of a curling rock cross the scratches produced by the front of the running band, at an angle due to the rotation of the curling rock, a sideways force will be exerted on them. It is shown that such a mechanism does lead to a curl distance of the correct magnitude and one that is insensitive to angular velocity. The model is then compared to previous experimental results where it is found to be in good agreement.

Keywords Curling · Ice friction · Scratch friction

1 Introduction

The game of curling involves sliding a 20-kg curling rock down a sheet of ice toward a target approximately 28 m away. The curler gives the rock some initial angular velocity as it is released which typically results in the rock undergoing between 1 and 4 rotations as it travels down the ice. The angular velocity causes the rock to deflect or curl away from the straight line path. The total amount of curl is approximately 1 m although it can vary from this value by as much as 30%. The direction of the curl is determined by the direction of the angular velocity. If the rock is rotating clockwise, as seen from above, it will curl to the right. If the rock is rotating counterclockwise, it will curl to the left. Up until now it has not been clear what is causing the curling rock to curl. A key feature is that the cause of the curl, the rotation of the curling rock, has very little impact on the amount of the curl. As long as the curling rock is given some initial angular velocity, it will curl approximately 1 m whether it undergoes one rotation or ten as it travels down the ice.

In order to try to understand the motion of a curling rock, some further details are needed. First the curling rock is not flat on the bottom but is curved so that only an annulus, called the running band, makes contact with the ice surface. The running band is approximately 6 cm in radius and is approximately 5 mm wide. Although the curling rock is polished granite, the running band is intentionally roughened. In addition, the ice surface itself is not smooth but is sprinkled with water so as to leave small ice pebbles on the surface. These ice pebbles are less than 1 mm in height and are a few mm in width. These ice pebbles greatly reduce the friction between the curling rock and the ice surface making it much easier to slide the rocks down the ice. Finally members of the team are allowed to sweep immediately in front of the curling rock which lowers the overall friction and increases the distance the rock travels before stopping.

There have been many attempts to explain why a curling rock curls. A review of the history of the scientific investigation of curling is provided by Lozowski et al. [1]. The most common explanations have been based on a front-back asymmetry for the friction force which is acting around the running band. The frictional force is generally taken to be normal Coulomb friction, i.e., friction which opposes the direction of motion. If the friction on the rear half of the running band is greater than that on the front half of the running band the rotating rock will deflect in the correct direction. Proposed models in this category include Johnson [2], Shegelski et al. [3–5]; Denny [6], and Maeno [7]. These models differ in the explanation of why the friction along the rear of the running band is greater. Maeno [8] provides a brief review of some of these models and concludes that more experimental measurements are needed. All the front-back asymmetry models suffer from the same two problems as discussed by Nyberg et al. [9]. First, even in the unrealistic case where all of the frictional force is confined just

✉ A. Raymond Penner
raymond.penner@viu.ca

[1] Department of Physics, Vancouver Island University, 900 Fifth Street, Nanaimo, BC V9R 5S5, Canada

to the rear half of the running band, the maximum amount of curl achievable by these models is approximately 0.5 m for the rotational velocities seen in the game. Second, in these front-back asymmetry models the amount that the rock curls is naturally found to depend on the angular velocity of the curling rock, which as stated is definitely not the case. Although this second problem can be overcome by having the distribution of the frictional force varying with angular velocity in the correct manner [6], the first problem still exists. A front-back asymmetry with normal Coulomb friction simply cannot explain the curl of a curling rock.

Other attempts have been based on a left–right asymmetry for the frictional force. The frictional force acting on a curling rock decreases with the rock's speed as has been directly measured [10, 11]. If a curling rock is rotating as it travels down the ice, then one side of the running band will be moving at a lower speed with respect to the ice than the other side. In the case of a counterclockwise rotation, this would be the left side when looking down. As the frictional force increases with decreasing speed, it then follows that the slower side will have a greater frictional force acting upon it. Unfortunately, the analysis shows that for Coulomb friction the resulting lateral frictional force acting on the front half of the running band is equal in magnitude and in the opposite direction to that acting on the back half. The left–right asymmetry with Coulomb friction leads to no net lateral force acting on the curling rock. Several models including Harrington [12], Denny [13] and Marmo and Blackford [14] have, however, attempted to explain the curl of the curling via the left–right asymmetry for the frictional force. For Harrington, it was more of a hypothesis as no model was provided. Marmo and Blackford's attempt is based on a combination of left–right asymmetry and front-back asymmetry. Details of their model are not provided, but the results they present show a strong dependence that the amount of curl has on the initial angular velocity of the curling rock which again is not found.

It can be concluded that Coulomb friction, whether combined with a left–right or a front-back asymmetry, cannot explain the curl of a curling rock. Ivanov and Shuvalov [15] demonstrated that removing the constraint of Coulomb friction and allowing the frictional force to have components both parallel and perpendicular to the velocity of the contact points can lead to a curl of the correct magnitude. Penner [11] previously hypothesized that the frictional force between the curling rock and the ice surface may be partly adhesive and therefore non-Coulomb in nature. As the rock is rotating, the adhesive nature of the force would be expected to cause a pivoting like action with the pivoting action greater along the slower side of the running band. This will result in a lateral deflection in the correct direction. In addition, given that the frictional force on the slow side of the rotating rock is greater this would also be expected to lead to a preferential pivoting about the slow side. Unfortunately, attempts to model the preferential pivoting by the author inevitably lead to a curl which increases with the angular velocity of the rock, again in disagreement with the experimental results. Recently Shegeleski and Lozowski [16] have proposed a model based on the above general pivoting hypothesis and have given some possible physical mechanisms that may lead to the adhesive nature.

An entirely new model of why a curling rock curls has been proposed by Nyberg et al. [10]. They propose that it is the scratching of the top of the pebbles by the asperities of the roughened running band that is the key to explaining why a curling rock curls. The reasoning behind Nyberg et al.'s proposal is based on experimental measurements that they undertook. First they determined the topography of an ice pebble before and after a curling rock passed over it. The surface of the pebble was found to be severely scratched by the roughened running band. This is a key result for the curling problem for it is the first time that the effect that a curling rock has on the surface of the ice has been measured. Nyberg et al. also found that the net friction acting on a curling rock with a polished running band, which did not curl, was much less than that of a normal curling rock. They postulated that the frictional difference between these two is due to the scratching. Finally, they carried out experiments with non-rotating curling rocks sliding over pre-scratched ice. The curling rock with the roughened band was deflected, while the curling rock with the polished running band was not.

As a result of these experimental results, Nyberg et al. postulate that when the asperities around the rear of the running band cross the scratches produced by the front of the running band, at an angle due to the rotation of the curling rock, a sideways force will be exerted on them. They provide estimates of what this sideways force would need to be to lead to the correct amount of curl and show that their proposal is plausible. They further provide reasons why the resulting net force will not depend on angular velocity. However, they do not provide a model to go along with their reasoning and do not actually determine what actual curling rock paths would be expected.

Further analysis of the scratches created along the tops of pebbles created by curling rocks was performed by Honkanen et al. [17]. By directly scanning the ice surface with a white light interferometer, cross-scratches caused by the leading and trailing sections of the curling rock's contact band were clearly observed. The scratch angle difference between the scratches caused by the leading and trailing sections were found to be consistent with the local velocity vectors along the annulus for various combinations of longitudinal and rotational speeds. It was hypothesized that for small scratch angle differences the transverse acceleration of the rock would be directly proportional to the scratch angle difference. Comparisons between the resulting theoretical

scratch angle difference—sliding time relationship and a typical experimental transverse velocity–time relationship indicated a correlation between the curl and the scratch angle difference. It was concluded that the dominating contribution responsible for the curl of a curling rock is given by the scratch-guide mechanism in support of Nyberg et al.

It is the goal of this manuscript to provide a model to go along with Nyberg et al.'s postulate. It will be shown that indeed the scratching of the pebbles by the running band does lead to the curling rock curling in the right direction with the correct amount of curl. In addition, the model leads to the amount of the curl being independent of the angular velocity of the curling rock. The modeled results will also be compared with experimental results produced by previous researchers.

2 Theory

2.1 Forces on Individual Asperities

To provide a model to go along with Nyberg et al.'s postulate, the frictional force acting on individual asperities, as they plow over the tops of the pebbles, needs to be determined. Although asperities would be expected to come in a variety of shapes, to keep things somewhat simple they will be modeled as having a circular cross section. The sideways and overhead view of an individual asperity scratching the top of an ice pebble is shown in Fig. 1. In this figure, the asperity is taken as being conical in shape with D being the diameter of the asperity at the surface of the pebble, h being the depth of the scratch, and R being the radius of the top of the pebble.

Given that there is no acceleration in the vertical direction the net force acting on any asperity will be parallel to the ice surface. Consider first the forces acting on a horizontal slice of the asperity, specifically a disc of radius r and thickness dz, as is shown in Fig. 1a. It is postulated that the pressure distribution acting around the disc as it plows through and fractures the ice can be approximated by

$$\sigma = \sigma_o \sin\theta \tag{1}$$

where σ_o will in general depend on the velocity of the disc. The pressure distribution is shown in Fig. 2 with respect to y'' and x'', axes parallel and perpendicular to the velocity of the disc. Although no experimental evidence is provided for (1), the general behavior seems plausible. The shear stress parallel to the disc's surface will be taken to be much less than the pressure exerted on the disc and will be neglected in the model. The resulting components of the force acting on the disc as it plows through ice will therefore be;

$$df_{d,y''} = -\int_o^{\pi} \left(\sigma_o \sin\theta\right) \sin\theta \; r \, \mathrm{d}\theta \, \mathrm{d}z = -\frac{\pi}{2} \sigma_o r \, \mathrm{d}z, \tag{2a}$$

and

$$df_{d,x''} = \int_o^{\pi} \left(\sigma_o \sin\theta\right) \cos\theta \; r \, \mathrm{d}\theta \, \mathrm{d}z = 0. \tag{2b}$$

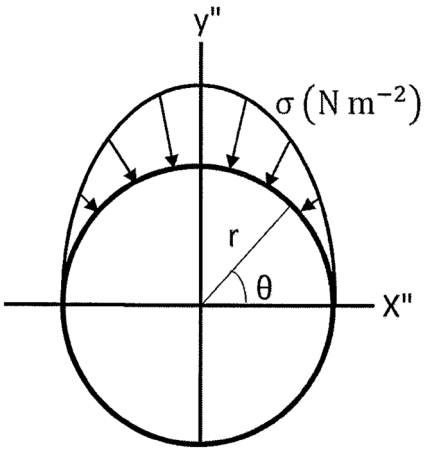

Fig. 2 Pressure distribution acting around a disc plowing through ice

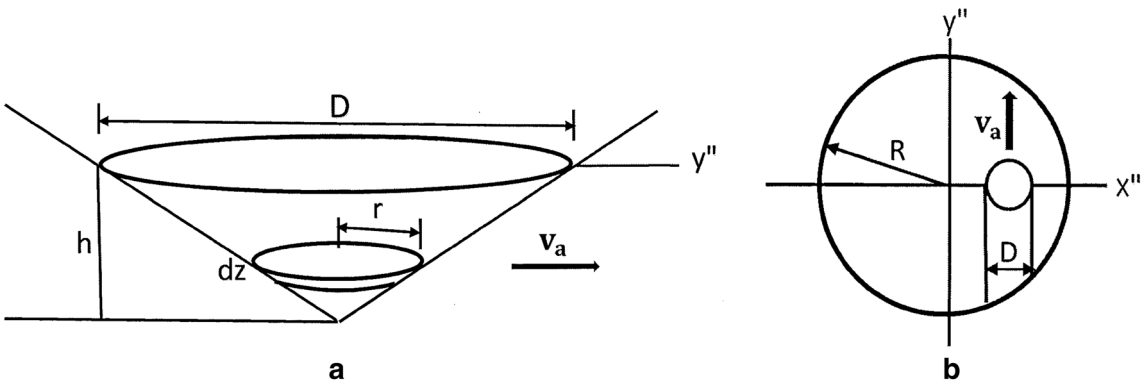

Fig. 1 An asperity crossing over the top of a pebble with a velocity $\boldsymbol{v}_a$; **a** side view, **b** top view. D is the diameter of the asperity at the surface of the pebble, h is the depth of the scratch, and R is the radius of the pebble

Consider now the case where the asperity crosses a previous scratch. This is shown in Fig. 3 where the attack angle, the angle the velocity of the asperity makes with the scratch, is given by φ. Figure 3a shows the disc as it crosses through the leading scratch wall. For this stage, the net lateral force will be in the positive x'' direction. When the disk passes into the far wall, Fig. 3b–f, the net lateral force will be in the negative x'' direction. The forces acting during these two stages are symmetric and in opposite directions and would be expected to lead to there being no net lateral force. However, if the asperity is conical or even irregularly shaped, it would be expected that as the asperity first makes contact with the leading scratch that the ice wall would fracture in the immediate vicinity of the initial contact point. As the neighboring sections of the asperity then pass through the wall, the pressure exerted by the wall on these sections would be expected to be greatly reduced. Overall the pressure exerted on a given disc by the ice during the stage shown in Fig. 3a would be expected to be much less than the pressure exerted on the disc as it passes into the far wall. As an approximation the lateral force due to the disc crossing the leading scratch wall will therefore be neglected in the model.

The lateral force acting on the disc as it passes through the far wall itself involves two stages. The first stage starts from $t=0$, corresponding to Fig. 3b when the disc first makes contact with the wall with $\theta_1=\theta_2=\varphi$, and ends when $t=T_1$, corresponding to Fig. 3d when θ_1 reaches a value of 0. From the geometry, it is found that during this stage:

$$\theta_1 = \phi - \cos^{-1}\left(1 - \frac{v_a t}{r}\sin\phi\right), \tag{3a}$$

$$\theta_2 = \phi + \cos^{-1}\left(1 - \frac{v_a t}{r}\sin\phi\right), \tag{3b}$$

and

$$T_1 = \frac{r(1-\cos\phi)}{v_a \sin\phi} \tag{4}$$

where v_a is the speed of the disc and asperity. The resulting lateral impulse acting on the disc during this stage will therefore be

$$dI^1_{d,x''} = -\int_0^{T_1}\int_{\theta_1}^{\theta_2}\left(\sigma_o \sin\theta\right)\cos\theta \; r \, d\theta \, dt \, dz \tag{5a}$$

$$= -\frac{1}{2} r \, \sigma_o \int_0^{T_1}\left(\sin^2\theta_2 - \sin^2\theta_1\right) dt \, dz. \tag{5b}$$

Substituting from (3a, 3b) and (4) and carrying out the integration in (5b) leads to

$$dI^1_{d,x''} = -\frac{2\sigma_o r^2}{3v_a}\cos\phi \, \sin^3\phi \, dz. \tag{6}$$

The second stage starts from $t=T_1$ and ends when $t=T_2$, corresponding to the disc going from Fig. 3d–f when θ_2 reaches π. From the geometry, it is found that during this stage;

$$\theta_1 = 0, \tag{7a}$$

$$\theta_2 = \phi + \cos^{-1}(\cos\phi - \frac{v_a(t-T_1)}{r}\sin\phi, \tag{7b}$$

and

$$T_2 = T_1 + \frac{2r\cos\phi}{v_a \sin\phi} \tag{8a}$$

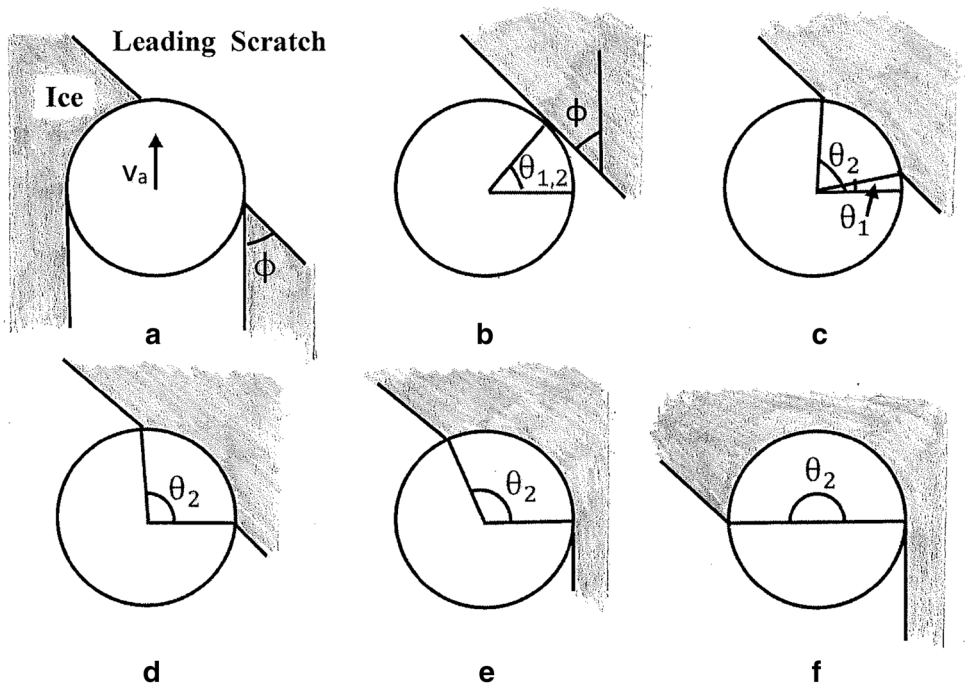

Fig. 3 Stages for a disc as it crosses a scratch

$$= \frac{r(1+\cos\phi)}{v_a \sin\phi}. \tag{8b}$$

The resulting lateral impulse acting on the disc during this stage is therefore

$$dI^2_{d,x''} = -\int_{T_1}^{T_2}\int_0^{\theta_2} \left(\sigma_o \sin\theta\right)\cos\theta \; r \; d\theta \; dt \; dz \tag{9a}$$

$$= -\frac{1}{2} r \; \sigma_o \int_{T_1}^{T_2} \left(\sin^2\theta_2\right) dt \; dz \tag{9b}$$

Substituting from (7a, 7b) and (8b) and carrying out the integration in (9b) leads to

$$dI^2_{d,x''} = -\frac{2\sigma_o r^2}{3 v_a \sin\phi}\cos\phi\left(1-\sin^4\phi\right) dz \tag{10}$$

During the time, it takes an asperity to cross a pebble it will cross an average of

$$N_s = \frac{\overline{\Delta y''}}{s}\sin\phi \tag{11}$$

scratches where s is the average center to center separation of the scratches on the pebble made by the front half of the running band and $\overline{\Delta y''}$, the average crossing distance for an asperity, is given by

$$\overline{\Delta y''} = \frac{\int_{-R}^{R}\left(R^2-y^2\right)^{1/2} dy}{2R} = \frac{\pi}{2}R \tag{12}$$

with R being the radius of a pebble. Therefore, the total lateral impulse exerted on the disc during a crossing of a pebble will by (6) and (10–12) be given by

$$dI_{d,x''} = N_s(dI^1_{d,x''} + dI^2_{d,x''}) \tag{13a}$$

$$= -\frac{\pi\sigma_o R r^2}{3 v_a s}\cos\phi \; dz. \tag{13b}$$

The average lateral force that is exerted on the disc over the time that the asperity is crossing a pebble will therefore be

$$df_{d,x''} = \frac{dI_{d,x''}}{t_{cross}} \tag{14}$$

where t_{cross}, the average time it takes an asperity to cross a pebble is given by

$$t_{cross} = \frac{\overline{\Delta y''}}{v_a}. \tag{15}$$

Therefore by (12–15),

$$df_{d,x''} = -\frac{2\sigma_o \; r^2}{3s}\cos\phi \; dz. \tag{16}$$

Given the forces acting on a disc, the forces acting on an asperity of circular cross-section can be determined. First the geometry of the asperity needs to be specified. Two different geometries will be considered that will provide an expected range for these forces. These are an asperity with a conical shape and one with a cylindrical shape. For a conical shaped asperity, the dependence that the radius of the disc has on its location along the asperity is given by

$$r = \frac{D}{2h} z \quad h \geqslant z \geqslant 0. \tag{17}$$

where D is the width of the asperity at the surface of the pebble and h is the depth of the scratch. The components of the total force acting on such an asperity will therefore by (2a) and (16, 17) be given by

$$f_{a,y''} = \int_0^h df_{d,y''} \tag{18a}$$

$$= -\frac{\pi}{8}\sigma_o D \; h \tag{18b}$$

and

$$f_{a,x''} = \int_0^h df_{d,x''} \tag{19a}$$

$$= -\frac{1}{18s}\sigma_o D^2 \; h \cos\phi \tag{19b}$$

$$= \kappa \, f_{a,y''} \tag{19c}$$

where κ, defined as the ratio of the lateral and parallel force components acting on a asperity, is given by

$$\kappa = \frac{4}{9\pi}\left(\frac{D}{s}\right)\cos\phi. \tag{20}$$

For a cylindrical shaped asperity

$$r = D/2 \tag{21}$$

leading to

$$f_{a,y''} = -\frac{\pi}{4}\sigma_o D h \tag{22}$$

and

$$f_{a,x''} = \kappa \, f_{a,y''} \tag{23}$$

with

$$\kappa = \frac{6}{9\pi}\left(\frac{D}{s}\right)\cos\phi. \tag{24}$$

In this model, the maximum lateral force occurs when the angle φ equal to 0. This corresponds to the case where the asperity is travelling parallel to the given scratch but with half of it imbedded in the ice.

Using (20) and (24) as an estimate for the range of the ratios of lateral and parallel forces acting on asperities of circular cross-section then leads to

$$\kappa = \left(\eta \frac{D}{s}\right)\cos\phi \tag{25}$$

where

$$0.14 < \eta < 0.21. \tag{26}$$

Equations (19c) and (25) are a key result of the analysis. First, the average lateral force acting on an asperity as it passes over the pebble is directly proportional to the average parallel force acting on it. Second, the lateral force acting on an asperity just depends on the nature of the scratches. The lateral force depends on D/s, the ratio of the scratch width at the surface to the center to center separation of the scratches. This ratio is also equal to the fraction of the top of the pebble surface that is being scratched. The lateral force also depends on the shape of the asperities through the value of η. Only asperities with circular cross sections were considered but other shapes would be expected to lead to similar results. Finally the average lateral force acting on an asperity depends only weakly on the attack angle through the term cosφ.

The model will break down if T_2 as given by (8b) is greater than t_{cross}. In this case, a trailing asperity does not fully cross a scratch. This is important when the initial angular velocity of the curling rock is so low that the rock undergoes less than 1 rotation as it travels down the ice. Such low angular velocities are not found in the game except in the case where the curling rock is thrown at high speed in order to knock out the opposing teams curling rock(s). Such low angular velocities will not be considered.

2.2 Total Force Acting on the Curling Rock

Given (19c) and (25) the net force acting on all the asperities that are around the running band, and therefore the net force acting on the curling rock, can now be determined. Figure 4a shows the velocity of two asperities on opposite halves of a running band of radius ρ for a curling rock travelling with a translational velocity $\boldsymbol{v}_o$ and an angular velocity $\boldsymbol{\omega}$. With respect to a reference frame fixed to the curling rock, with y' in the direction of $\boldsymbol{v}_o$, the velocity of a given asperity located at an angular position α with respect to the x'-axis will be given by

$$\boldsymbol{v}_a = \boldsymbol{v}_o + \boldsymbol{\omega} \times \boldsymbol{\rho} \tag{27}$$

where

$$\rho = (\rho\ \cos\alpha)\hat{\boldsymbol{i}'} + (\rho\ \sin\alpha)\hat{\boldsymbol{j}'}. \tag{28}$$

Equations (27) and (28) lead to

$$\boldsymbol{v}_a = (-\omega\ \rho\ \sin\alpha)\ \hat{\boldsymbol{i}'} + \left(v_o + \omega\ \rho\ \cos\alpha\right)\hat{\boldsymbol{j}'} \tag{29}$$

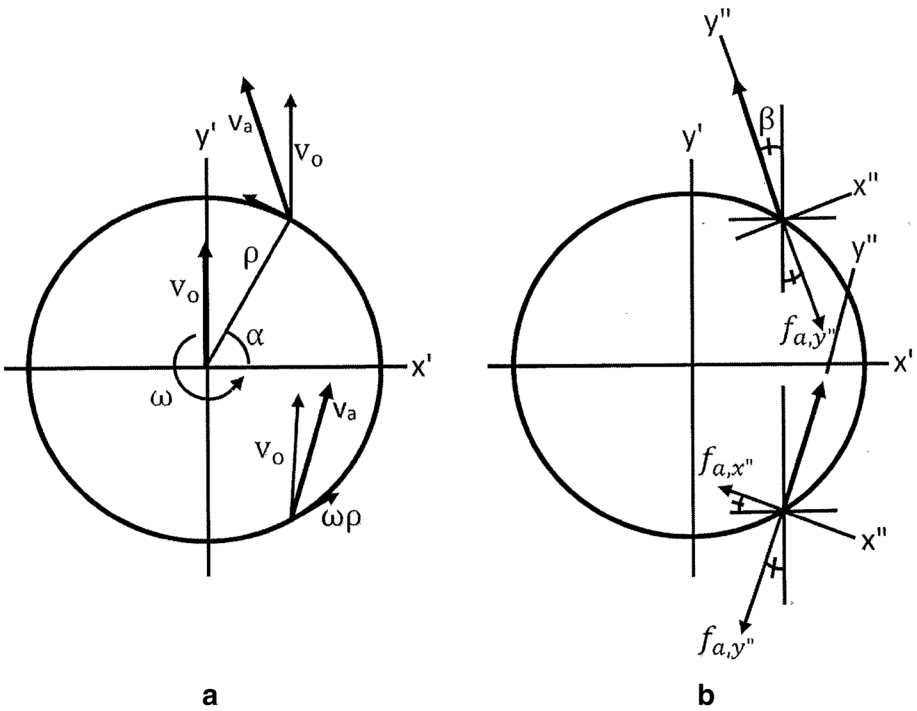

Fig. 4 The **a** velocity and **b** forces acting on two asperities on opposite halves of the running band

where $\hat{i}'$ and $\hat{j}'$ are the unit vectors in the $x'y'$ reference frame.

Figure 4b shows the forces acting on the two asperities. On the front half, only $f_{a,y''}$ will act while the back half will have, in addition to $f_{a,y''}$, the lateral force $f_{a,x''}$. With respect to the $x'y'$ reference frame, the components of the force acting on an asperity will be

$$f_{a,y'} = f_{a,y''}\cos\beta \quad 0 < \alpha < \pi \tag{30a}$$

$$= f_{a,y''}\cos\beta - f_{a,x''}\sin\beta \quad \pi < \alpha < 2\pi \tag{30b}$$

and

$$f_{a,x'} = -f_{a,y''}\sin\beta \quad 0 < \alpha < \pi \tag{31a}$$

$$= f_{a,x''}\cos\beta + f_{a,y''}\sin\beta \quad \pi < \alpha < 2\pi \tag{31b}$$

where β, the angle that the asperity's velocity makes with the y'-axis, is given by

$$\beta = \cos^{-1}\left(\hat{v}_{\mathbf{a}} \cdot \hat{j}'\right) \tag{32a}$$

$$= \cos^{-1}\left(\frac{v_{\mathrm{o}} + \omega\rho\,\cos\alpha}{v_{\mathrm{a}}}\right). \tag{32b}$$

The attack angle φ for the asperities on the back half of the running band will simply be

$$\phi = 2\beta. \tag{33}$$

Given that the width of the ice pebbles is only a few mm's, the attack angle can be taken to be the same for all the asperities that are crossing a given pebble. The specific attack angle for a given pebble being traversed by the back half of the running band will depend on the angular position α through Equations (32b) and (33).

Taking that the distribution of the asperities is uniform around the running band, the angular density of the asperities that are in contact with pebbles is given by

$$n_{\mathrm{a}} = \frac{N_{\mathrm{a}}}{2\pi} \tag{34}$$

where N_{a} is the total number of asperities in contact at any one time. Therefore, the y' component of the total force that is acting on the curling rock is, from (19c) and (30a, 30b), given by

$$\mathrm{F}_{y'} = \frac{N_{\mathrm{a}}}{2\pi}\int_0^{2\pi} f_{a,y'}\,\mathrm{d}\alpha \tag{35a}$$

$$= \frac{N_{\mathrm{a}}}{2\pi}\left[\int_0^{\pi} f_{a,y''}\cos\beta\,\mathrm{d}\alpha + \int_{\pi}^{2\pi}(f_{a,y''}\cos\beta - f_{a,x''}\sin\beta)\,\mathrm{d}\alpha\right] \tag{35b}$$

$$= \frac{N_{\mathrm{a}}}{2\pi}\left[\int_0^{2\pi} f_{a,y''}\cos\beta\,\mathrm{d}\alpha - \int_{\pi}^{2\pi} \kappa f_{a,y''}\sin\beta\,\mathrm{d}\alpha\right]. \tag{35c}$$

The x' component of the total force is in turn, from (19c) and (31a, 31b), given by

$$\mathrm{F}_{x'} = \frac{N_{\mathrm{a}}}{2\pi}\int_0^{2\pi} f_{a,x'}\,\mathrm{d}\alpha \tag{36a}$$

$$= \frac{N_{\mathrm{a}}}{2\pi}\left[-\int_0^{\pi} f_{a,y''}\sin\beta\,\mathrm{d}\alpha + \int_{\pi}^{2\pi}(f_{a,x''}\cos\beta + f_{a,y''}\sin\beta)\,\mathrm{d}\alpha\right] \tag{36b}$$

$$= \frac{N_{\mathrm{a}}}{2\pi}\int_{\pi}^{2\pi} \kappa f_{a,y''}\cos\beta\,\mathrm{d}\alpha. \tag{36c}$$

As shown by Eq. (36c), the x' component of the total force is directly proportional to κ, the proportionality constant between the lateral and parallel force components acting on an individual asperity on the back half of the running band as it crosses a scratch created by an asperity on the front half of the running band. If there was no lateral forces acting on the individual asperities, there would still be a net x' component of force acting on both the front half and the back half of the curling rock, but these forces would cancel as can be determined from Eq. (36b) if $f_{a,x''}$was set equal to zero.

In the special case where the curling rock has no angular velocity, both β and φ will be equal to 0 and from (35c)

$$\mathrm{F}_{y'} = N_a f_{a,y''}. \tag{37}$$

Equating (37) to

$$\mathrm{F}_{y'} = -\mu\mathrm{mg} \tag{38}$$

where μ is the coefficient of kinetic friction and m is the mass of the curling rock, leads to

$$\mu = -\frac{N_a f_{a,y''}}{\mathrm{mg}} \tag{39}$$

with $f_{a,y''}$ being negative in sign. Expressing (35c) and (36c) in terms of μ and substituting from (32b) then leads to

$$a_{y'} = \frac{F_{y'}}{m} = -\frac{g}{2\pi}\left[\int_0^{2\pi}\mu\left(\frac{v_{\mathrm{o}} + \omega\,\rho\,\cos\alpha}{v_{\mathrm{a}}}\right)\mathrm{d}\alpha + \int_{\pi}^{2\pi}\kappa\,\mu\left(\frac{\omega\,\rho\,\sin\alpha}{v_{\mathrm{a}}}\right)\mathrm{d}\alpha\right] \tag{40}$$

and

$$a_{x'} = \frac{F_{x'}}{m} = -\frac{g}{2\pi}\int_{\pi}^{2\pi}\kappa\,\mu\left(\frac{v_{\mathrm{o}} + \omega\,\rho\,\cos\alpha}{v_{\mathrm{a}}}\right)\mathrm{d}\alpha \tag{41}$$

where by (25), (32b) and (33)

$$\kappa = \left(\eta\frac{D}{s}\right)\cos\left(2\cos^{-1}\left(\frac{v_{\mathrm{o}} + \omega\rho\,\cos\alpha}{v_{\mathrm{a}}}\right)\right) \tag{42}$$

and by (29)

$$v_{\mathrm{a}} = \left((\omega\rho\,\sin\alpha)^2 + \left(v_{\mathrm{o}} + \omega\rho\,\cos\alpha\right)^2\right)^{1/2}. \tag{43}$$

The net torque acting on the curling rock is found in turn from

$$\boldsymbol{\tau}' = \frac{N_a}{2\pi}\int_0^{2\pi}\left(\boldsymbol{\rho} \times \left(f_{a,x'}\hat{\boldsymbol{i}}' + f_{a,y'}\hat{\boldsymbol{j}}'\right)\right)\mathrm{d}\alpha \tag{44a}$$

$$= \frac{N_a}{2\pi}\int_0^{2\pi}\rho(f_{a,y'}\cos\alpha - f_{a,x'}\sin\alpha)\,\mathrm{d}\alpha\,\hat{\boldsymbol{k}}'. \tag{44b}$$

Substituting from (30–31), and (32b) into (44b) then results in

$$\tau_z' = -\frac{mg}{2\pi}\left[\int_0^{2\pi}\mu\,\rho\left(\frac{v_o\cos\alpha + \omega\,\rho}{v_a}\right)d\alpha + \int_\pi^{2\pi}\kappa\,\mu\,\rho\left(\frac{v_o\,\sin\alpha}{v_a}\right)d\alpha\right] \tag{45}$$

Treating the rock as a cylinder with a radius of R_c results in a moment of inertia of $\frac{1}{2}\,mR_c^2$ and an angular acceleration of

$$\alpha_z' = -\frac{g}{\pi R_c^2}\left[\int_0^{2\pi}\mu\,\rho\left(\frac{v_o\cos\alpha + \omega\,\rho}{v_a}\right)\mathrm{d}\alpha + \int_\pi^{2\pi}\kappa\,\mu\,\rho\left(\frac{v_o\,\sin\alpha}{v_a}\right)\mathrm{d}\alpha\right]. \tag{46}$$

The final step is to transform (40–41), and (46) to a reference frame fixed to the ice surface. This leads to

$$a_y = a_x'\sin\psi + a_y'\cos\psi \tag{47a}$$

$$a_x = a_x'\cos\psi - a_y'\sin\psi \tag{47b}$$

$$\alpha_z = \alpha_z' \tag{47c}$$

where ψ, the rotation angle between the $x'y'$ frame of the curling rock and the xy frame of the ice surface, is given by

$$\psi = \cot^{-1}\left(\frac{\mathrm{d}y}{\mathrm{d}x}\right) \tag{48}$$

with $y(x)$ being the path of the curling rock along the ice surface.

2.3 The Coefficient of Kinetic Friction and the Value of ηD/s

Figure 5 shows the dependence that μ_o, the coefficient of friction, has on the sliding velocity for a curling rock, as determined by Nyberg et al. [10]. The behavior is similar to the previous results of Penner [11]. A least square fit to the data results in

$$\mu_o = 0.011 + \frac{0.0019}{v_o}. \tag{49}$$

Nyberg et al. also measured the coefficient of friction for a curling rock with a polished band. They found that in this case the coefficient was approximately constant with a value of 0.010.

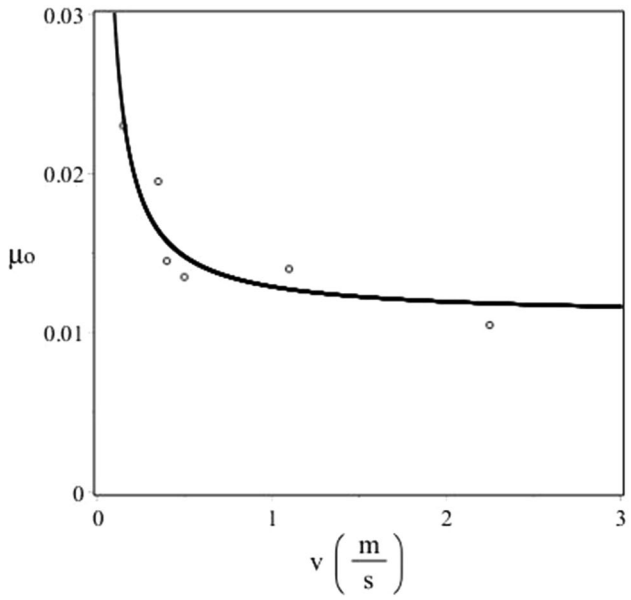

Fig. 5 Dependence that μ_o has on the sliding speed of the curling rock. o—data from Nyberg et al. [10]

Lozowski et al. [1] determined a theoretical value for μ_p, the coefficient of friction that is specifically due to asperities plowing through the ice. Treating the asperities as being conical in shape it was shown that

$$\mu_o = \frac{\alpha}{\pi} \tag{50}$$

where α, the asperity's aspect ratio, is equal to, for conical asperities, h/D. From a study of the topography of a scratched ice pebble, Nyberg et al. [10] estimated that for an average scratch, h ≅ 3 μm and D ≅ 50 μm. Therefore by (50) $\mu_p \cong 0.019$. Comparing this value for μ_p to Fig. 5, it is concluded that the frictional force acting on a curling rock is dominated by the forces exerted on the asperities as they plow through the top of a pebble and fracture the ice.

Nyberg et al. postulated that it is the difference between the frictional force for a curling rock with a roughened band and one with a polished band that is due to the scratching. In the model presented in this manuscript, it is taken that this is not the case and that μ_o as given by (49), and for all the velocities found in the game, is dominated by the frictional forces acting on the asperities as they fracture the ice. The results for a curling rock with a polished band cannot be extrapolated to one with a roughened band. The primary source of the frictional force could be very different.

In general, the frictional force would be expected to be different for the ice sheets at different curling rinks. To take

this into account, the coefficient of friction in the model will be taken to be given by

$$\mu = \gamma \mu_o \tag{51}$$

where γ gives the relative friction between a given ice surface and the particular one that Nyberg et al. collected their data on.

The value of D/s also needs to be determined for the model. On Fig. 5a, b in Nyberg et al. [10] the topography of the running band and the cross section of the surface of a pebble before and after a curling rock has crossed it are shown. From the figures, it would appear that almost all of the surface of the pebble is being scratched by the running band. Indeed it appears that it is more that the pebble surface is being scrapped along its top. Considering that D/s in the model is equivalent to the actual fraction of the top of the pebble that is being scratched this would lead to a high value for D/s. However, there is a complication, in that the figures shows the topography after both the front and the back of the running band have crossed the pebble surface. In the model, D/s applies to only after the front half has passed. As such the following wide estimated range will be used in the model

$$0.5 \leqslant D/s \leqslant 1.0, \tag{52}$$

where the value of 1.0 corresponds to the maximum possible value.

From the figures in Nyberg et al. [10], it appears that the shape of any distinct asperities and scratches tend toward being conical. For some sections of the pebble's surface the geometry of the scratches is not so clear. Also given that asperities will often deviate from the circular cross section in the model the wide range for η as given by (26) will be used. Combining the two parameters that relate to the nature of the scratching (26) and (27), then leads to the following range

$$0.07 \leqslant \eta D/s \leqslant 0.21. \tag{53}$$

3 Results

Given Eqs. (40–41), (46–48), along with (25) and values for γ and $\eta D/s$, the motion of a curling rock sliding down an ice sheet can be determined. Figure 6 shows the modeled paths for a curling rock with an initial velocity of 2.6 m/s, an initial angular velocity of 1.5 rad/s, and with γ set equal to 1. These values lead to the curling rock stopping after 19.9 s after travelling 28.0 m down the ice sheet and undergoing a total of 2.7 revolutions, typical values found in the game. The values for $\eta D/s$ which are being used are the limits as given by (53), corresponding to the minimum and maximum amount of curl obtained from the model. The resulting curl distances found are 0.44 m for $\eta D/s = 0.07$ and 1.33 m for $\eta D/s = 0.21$. Given the approximations and simplifications made in the model, the result is quite good. Scratch friction

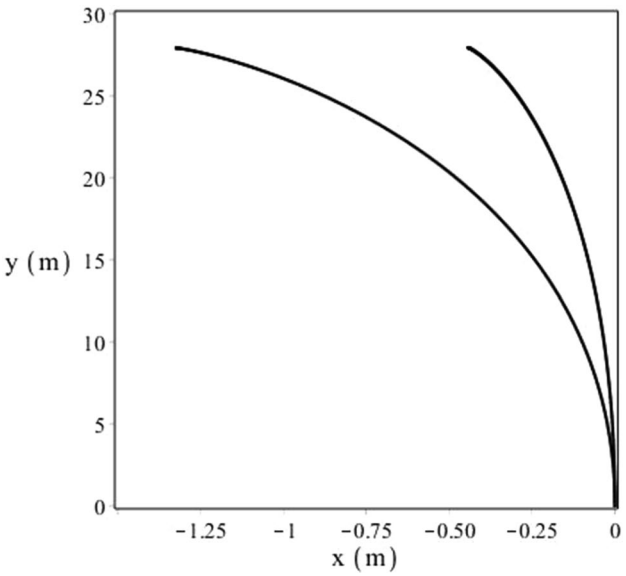

Fig. 6 Path of a curling rock with the minimum and the maximum curl as determined by the model

and the resulting lateral force can lead to a curl of the right magnitude.

The magnitude of the curl obtained from the model fundamentally falls out from the relationship as given by (25) as κ will have, for an average value of 0.14 for $\eta D/s$ and with $\cos\varphi \cong 1$, a value of approximately 0.14. This leads by (40–41) and neglecting the second term of (40) as $\kappa << 1$, to

$$a'_x \cong \frac{\kappa}{2} a'_y \tag{54a}$$

$$\cong \frac{1}{14} a'_y. \tag{54b}$$

Given that the parallel and lateral accelerations are applied over the same time interval and that the rock travels approximately 28 m down the ice, this leads to, assuming constant acceleration, an expected curl distance of approximately 2 m. Transforming to the reference frame of the ice via (47), however, leads to the actual curl with respect to the ice surface being closer to 1 m.

Consider now the dependence that the amount of curl in the model has on the angular velocity of the curling rock. In Fig. 7 are the experimental results from Penner [11] and Jensen and Shegelski [18]. As is seen the curl distance is approximately independent of the number of rotations that the curling rock undergoes as it slides down the ice. The scatter is large, partially due to the experimental technique, with the amount of the curl ranging between 0.7 and 1.3 m. The slight drop of curl distance with number of rotations that is seen would appear to be a real effect as high-precision measurements by Hattori et al. [19] also show that the curl

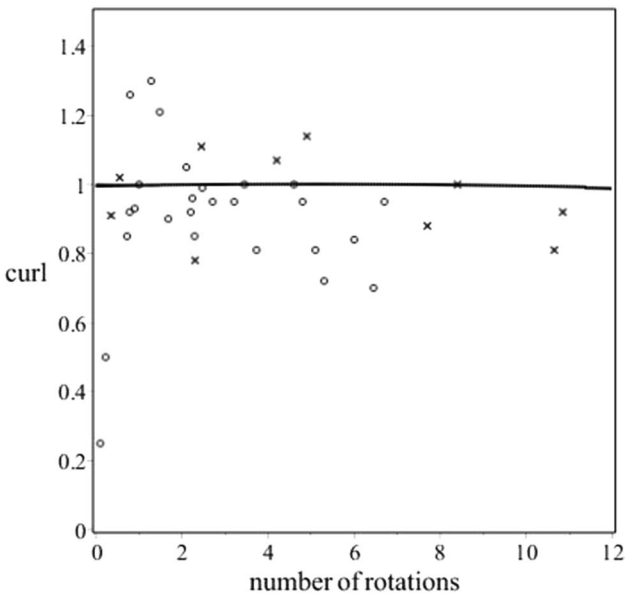

Fig. 7 Dependence of the magnitude of the curl versus the number of rotations the curling rock makes as it slides down the ice. *o*—data from Penner [11], *x*—data from Jensen and Shegleski [18]

distance decreases with the number of rotations with values in their case dropping from nearly 1.4 m for 1 rotation to 0.9 m for 10 rotations. Figure 7 includes the modeled dependence that the curl has on the total number of revolutions. In the model, the initial sliding velocity and γ were set at 2.6 ms^{-1} and 1, respectively, so that the rock stops after travelling 28 m. The value of η*D*/*s* was set to 0.152 so that the amount of curl is approximately equal to 1.0 m. There is a slight dependence that the distance traveled has on the angular velocity, however, this effect is very small, i.e., < 1%, and was not corrected for. As is seen, the model leads to a nearly constant amount of curl which is in reasonable agreement with the experimental results. The total amount that the rock curls in the model has virtually no dependence on the number of rotations that the curling rock undergoes.

The reason for this insensitivity to angular velocity in the model stems again from the expression for κ, as given by (25), for the dependence that the lateral acceleration has on angular velocity comes primarily from the dependence that κ has on cosφ. Even for the rock undergoing ten rotations as it travels down the ice the maximum value of φ around the running band is only approximately 20°. Curlers will throw the rock with an initial angular velocity that is comfortable to them as it makes little difference to the amount that the rock curls. On a more fundamental level, the insensitivity to angular velocity comes from (10) and (11). The average lateral impulse acting on a scratch crossing asperity for relativity small attack angles is approximately proportional to sinφ, while the average number of scratches crossed by the asperity is proportional to $(\sin\varphi)^{-1}$. These effects cancel.

As stated in Sect. 2.1, the model starts to break down if the initial angular velocity is so low that the curling rock executes less than 1 rotation as it travels down the ice. Previously when collecting the data shown in Fig. 7, the author found that curling rocks thrown with such little angular velocity will often stop rotating well before coming to rest. Therefore, for both the model and in practice the curling rock needs to be thrown with enough initial angular velocity so that it undergoes at least approximately 1 rotation before coming to rest.

To compare the model with experimental results, data from Jensen and Shegelski [18] were used. By using a video camera, they determined the *x, y*, and angular positions of a curling rock frame by frame. Their curling rock travelled 25.6 m down the ice in 22.8 s, curled 0.78 m and underwent approximately 2.7 rotations. Using the initial position and time points of their data set, the initial velocity of their curling rock is estimated to be 2.09 m s^{-1} and the initial angular velocity is estimated at -1.01 rad s^{-1}. The relative friction for their specific ice sheet, γ, was set at 0.688 so that for the initial velocity the rock traveled 25.6 m down the ice before stopping. Therefore, in their case the friction of their ice sheet was less than that in the case of Nyberg et al. Using the scratch model, the curling rock was found to take 22.4 s to travel down the ice which compares well with the experimental value of 22.8 s. The value of η*D*/*s* was set so that the rock curled a lateral distance of 0.78 m in agreement with the experimental results. The value found for η*D*/*s* was 0.132, near the middle of the range given by (53). Figure 8a–c shows the resulting *x, y*, and angular positions of the rock versus time for both the experimental data and the model. Figure 8d shows the modeled trajectory compared to the experimental trajectory. As seen in Fig. 8b, d the modeled values for the x position of the rock overshoot the experimental values. However, the difference is less than ~ 5 cm which is relatively small as compared to the curling rock itself which has a diameter of 28 cm. The modeled angular position on the other hand undershoots the experimental values. However, the modeled results being presented are based on the estimates for the initial velocities. As an example of the effect Fig. 8c also includes the modeled case where the initial angular velocity is 7% greater, i.e., − 1.07 rad s^{-1}. For this slightly greater value, the agreement between the model and the experimental results is seen to be much better. Also the dependence that the friction has on velocity for the given ice surface may be different than that as given by (49), which would also be expected to lead to differences. Overall the modeled results are in good agreement with the experimental results.

As another comparison of the model with experimental results, the results of Lozowski et al. [20] were used. In this case, a curling rock was equipped with an inertial measurement unit (IMU) allowing for the determination

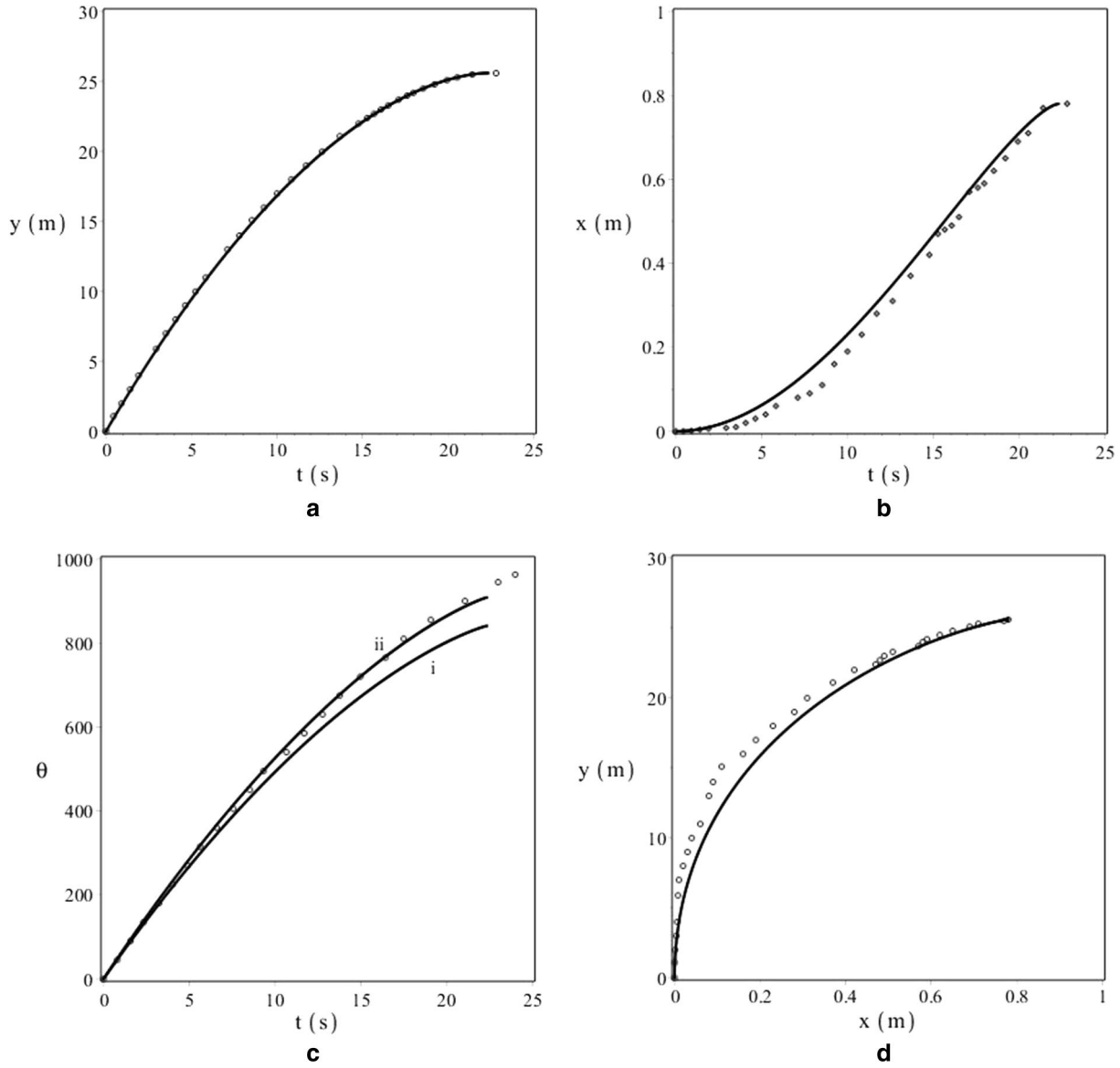

Fig. 8 Comparison of the modeled results with the experimental results of Jensen and Shegelski [18]. For **c**, i—using Jensen and Shegleski's initial angular velocity of -1.01 rad/s, ii—using an initial angular velocity of -1.07 rad/s

of the linear and angular velocity components. For their curling rock, the initial linear and angular velocities were 2.15 ms^{-1} and 1.6 rad s^{-1}, respectively, and the rock travelled for 21.9 s before coming to rest. In the model, γ was set to 0.73 to have the same stopping time for the given initial velocity. Their curling rock had a total curl of 1.21 m. The value of ηD/s was set to 0.204 in the model to agree with this net lateral displacement. The resulting dependence that the velocity components have on time as provided by the model are shown in Fig. 9a-c along with the IMU results of Lozowski et al. The results are mixed. As seen in Fig. 9a, the modeled y-component of the velocity is in good agreement with the IMU results. The x-component of the velocity results, as shown in Fig. 9b, is not so clear. The IMU x-component of the velocity has a jump from 0 to a maximum magnitude of 0.10 m s^{-1} at approximately the 8 s mark after which it stays constant for approximately another 8 s before dropping back down to 0. This would seem to indicate that a single event, happening at approximately the 8 s mark, is responsible for the lateral deflection. This behavior does not agree with previous observations and measurements of the motion of curling rocks. However, even given this qualifier, the general behavior of the x-component of the velocity as provided by the model, which would seem to be much more reasonable behavior, is not that far off the IMU results.

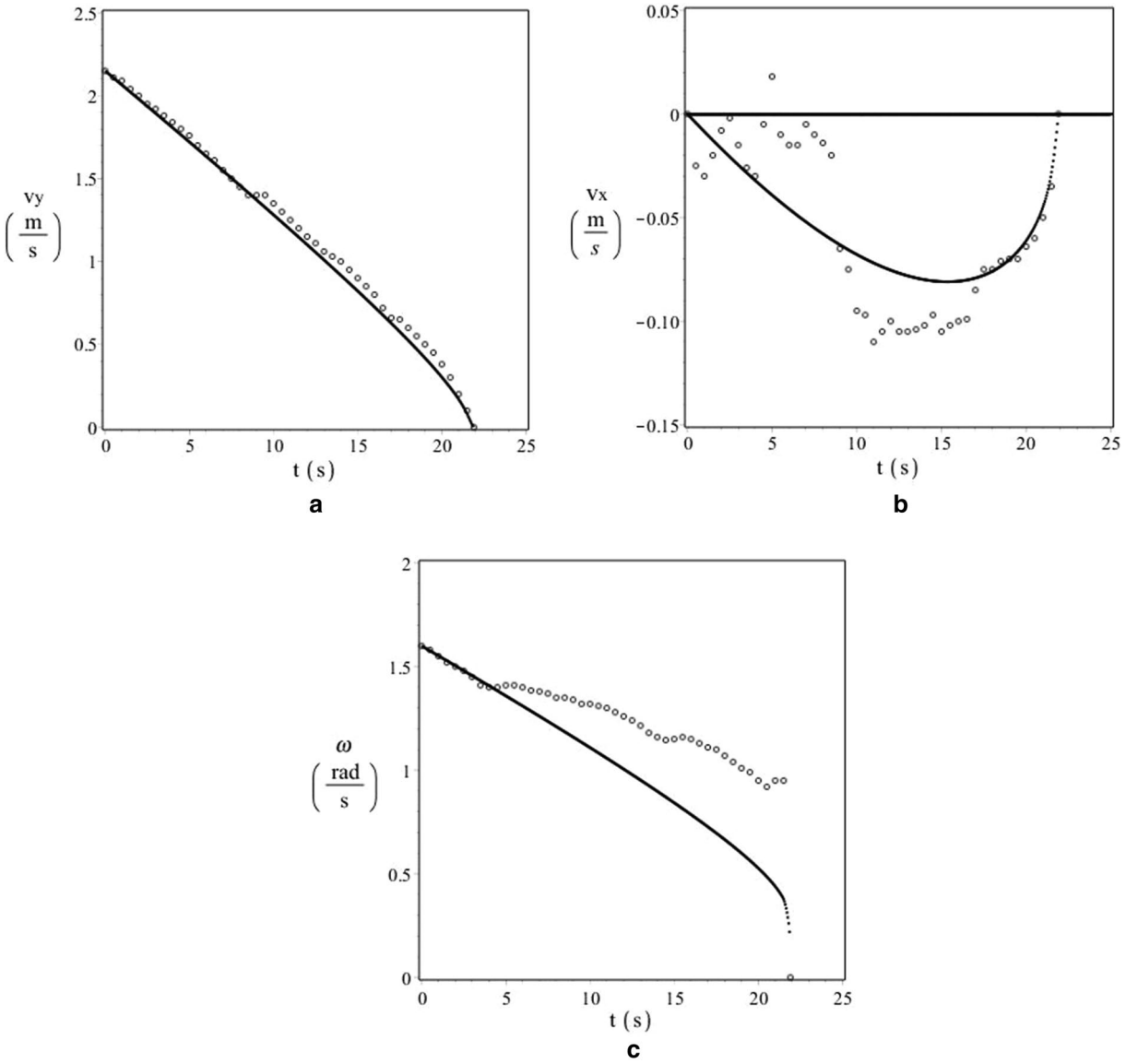

Fig. 9 Comparison of the modeled results with the IMU results of Lozowski et al. [20]

The modeled angular frequency shown in Fig. 9c significantly undershoots the IMU values. It is believed that before any conclusions are made regarding this difference further IMU data should be obtained. Figure 9c does show that, for both the model and the experimental data, the angular velocity of the curling rock falls off more slowly than the linear velocity, i.e., Figure 9a. As such, in some cases the velocity of the running band on the slow side of the curling rock will drop to zero, i.e., $v_o = \omega\rho$, prior to the rock coming to rest. In this case, the resulting large static friction at that point will cause the rock to pivot about this point just before it comes to rest. This is sometimes observed in the game.

4 Conclusion

The model presented in this manuscript includes many simplifications and approximations. Some of these will lead to a smaller curl, and some of these will lead to a greater curl. However, it is expected that even a more detailed analysis will lead to the same general result, namely that the average lateral force acting on an asperity, around the back half of the running band, as it crosses a pebble is proportional to the average parallel force acting upon it. If this is the case, it is expected that magnitude of

the curl and the insensitivity of the magnitude to angular velocity will be similar to what is presented here.

Shegelski and Lozowski [21] have pointed out that if the running band is so severely scratching the ice it would be expected that when the next thrown curling rock runs over the previously scratched pebbles it will undergo unexpected deflections. However, given that previous scratches left by the front and back halves of the running band of the curling will be symmetrical with respect to the y'-axis, the net lateral force that they would exert on the front and back halves of a subsequent curling rock will cancel out. Only in the case of asperities crossing a set of asymmetrical scratches, such as with Nyberg et al.'s test or with the back half of the running band crossing over the scratches produced by the front half, will there be a net lateral force. One suggested experiment would be to find the effect of asymmetrically scratched ice on the subsequent motion of a curling rock. It would be expected that the curl would be greater when the rock curls in the direction of the pre-scratched ice (i.e., for a rock curling clockwise when looking down the pre-scratches would tilt upwards from left to right) and will curl less when the rock is curling in the direction opposed to the pre-scratches.

Also, it is important to note that the surface of the pebble is being worn down by the passage of the curling rocks and is why the ice needs to be re-pebbled between games. The depths of any previous scratches are therefore probably not as deep as the ones left by the front half of a given curling rock. This is a hypothesis which can only be answered by experiments in line with what Nyberg et al. and Honkanen et al. have previously performed.

Even though questions may still remain, Nyberg et al. have shown experimentally that a curling rock does severely scratch the tops of the pebbles and that a scratched ice surface will deflect a curling rock. The theoretical results presented in this manuscript show that a model based on such scratching can lead to a curl of the correct magnitude and one that is insensitive to angular velocity. It is concluded that Nyberg et al.'s postulate of why a curling rock curls is plausible.

Acknowledgements E.T. Jensen, M.R.A. Shegelski, and E.P. Lozowski are thanked for providing the experimental data that was used for Figs. 8 and 9.

References

1. Lozowski, E.P., Szilder, K., Maw, S., Morris, A., Poirier, L., Kleiner, B.: Towards a first principles model of curling ice friction and curling stone dynamics. In: Proceedings of the twenty-fifth International Ocean and Polar Engineering Conference, USA, June 21–26, pp. 1730–1738 (2015)
2. Johnson, G.W.: The dynamics of a curling stone. Can. Aeronaut. Space J. **27**, 144–160 (1981)
3. Shegelski, M.R.A., Niebergall, R., Watton, M.A.: The motion of a curling rock. Can. J. Phys. **74**, 663–670 (1996)
4. Shegelski, M.R.A., Reid, M., Niebergall, R.: The motion of rotating cylinders sliding on pebbled ice. Can. J. Phys. **77**, 847–862 (1999)
5. Shegelski, M.R.A.: The motion of a curling rock: analytical approach. Can. J. Phys. **78**, 857–864 (2000)
6. Denny, M.: Curling rock dynamics: towards a realistic model. Can. J. Phys. **80**, 1005–1014 (2002)
7. Maeno, N.: Curl mechanism of a curling stone on ice pebbles. Bull. Glaciol. Res. **28**, 1–6 (2010)
8. Maeno, N.: Assignments and progress of curling stone dynamics. Proc. IMechE Part P. 1–6 (2016)
9. Nyberg, H., Hogmark, S., Jacobson, S.: Calculated trajectories of curling stones under asymmetrical friction: validation pf published models. Tribol. Lett. **50**, 379–385 (2013)
10. Nyberg, H., Alfredson, S., Hogmark, S., Jacobson, S.: The asymmetrical friction mechanism that puts the curl in the curling stone. Wear **301**, 583–589 (2013)
11. Penner, A.R.: The physics of sliding cylinders and curling rocks. Am. J. Phys. **69**, 332–339 (2001)
12. Harrington, E.L.: An experimental study of the motion of curling stones. Trans. Proc. R. Soc. Can. **8**, 247–259 (1924)
13. Denny, M.: Curling rock dynamics. Can. J. Phys. **76**, 295–304 (1998)
14. Marmo, B.A., Blackford, J.R.: Friction in the sport of curling. In: Proc. 5th Int. Sports Eng. Conf, pp. 379–385: (2004)
15. Ivanov, A.P., Shuvalov, N.D.: Friction in curling game. Preprints MATHMOD 2012 Vienna (2013)
16. Shegelski, M.R.A., Lozowski, E.P.: Pivot-slide model of the motion of a curling rock. Can. J. Phys. **94**, 1305–1309 (2016)
17. Honkanen, V., Ovaska, M., Alava, M.J., Laurson, L., Tuonenen, A.J.: A surface topography analysis of the curling stone curl mechanism. Sci. Rep. **8**, 8123 (2018)
18. Jensen, E.T., Shegelski, M.R.A.: The motion of curling rocks: experimental investigation and semi-phenomenological description. Can. J. Phys. **82**, 791–809 (2004)
19. Hattori, K., Tokumoto, M., Kashiwazaki, K., et al.: In: Proceedings of the Japanese Society of Mechanical Engineering (JSME) Symposium on Sports and Human Dynamics, Japan, October 29–31, 14, (2014)
20. Lozowski, E.P., Maw, S., Kleiner, B., Szilder, K., Shegelski, M., Musilek, P., Ferguson, D.: Comparison of IMU measurements of curling stone dynamics with a numerical model. Procedia Eng. **147**, 596–601 (2016)
21. Shegelski, M.R.A., Jensen, E.T., Reid, M.: Comment on the asymmetrical friction mechanism that puts the curl in the curling stone. Wear **69**, 336–337, (2015)